THE JOURNAL OF BIOLOGICAL CHEMISTRY VOL. 291, NO. 52, pp. 26850–26859, December 23, 2016
Published in the U.S.A.

Rapid Renal Regulation of Peroxisome Proliferator-activated Receptor γ Coactivator-1α by Extracellular Signal-Regulated Kinase 1/2 in Physiological and Pathological Conditions*

Received for publication, August 20, 2016, and in revised form, November 8, 2016 Published, JBC Papers in Press, November 14, 2016, DOI 10.1074/jbc.M116.754762

Justin B. Collier[‡1], **Ryan M. Whitaker**[‡], **Scott T. Eblen**[§], **and Rick G. Schnellmann**[‡¶2]

From the Departments of [‡]*Drug Discovery and Biomedical Sciences and* [§]*Cell and Molecular Pharmacology, Medical University of South Carolina, Charleston, South Carolina 29425 and the* [¶]*Ralph H. Johnson Veterans Administration Medical Center, Charleston, South Carolina 29425*

Edited by John Denu

Previous studies have shown that extracellular signal-regulated kinase 1/2 (ERK1/2) directly inhibits mitochondrial function during cellular injury. We evaluated the role of ERK1/2 on the expression of peroxisome proliferator-activated receptor γ coactivator-1α (PGC-1α) gene, a master regulator of mitochondrial function. The potent and specific MEK1/2 inhibitor trametinib rapidly blocked ERK1/2 phosphorylation, decreased cytosolic and nuclear FOXO3a/1 phosphorylation, and increased PGC-1α gene expression and its downstream mitochondrial biogenesis (MB) targets under physiological conditions in the kidney cortex and in primary renal cell cultures. The epidermal growth factor receptor (EGFR) inhibitor erlotinib blocked ERK1/2 phosphorylation and increased PGC-1α gene expression similar to treatment with trametinib, linking EGFR activation and FOXO3a/1 inactivation to the down-regulation of PGC-1α and MB through ERK1/2. Pretreatment with trametinib blocked early ERK1/2 phosphorylation following ischemia/reperfusion kidney injury and attenuated the down-regulation of PGC-1α and downstream target genes. These results demonstrate that ERK1/2 rapidly regulates mitochondrial function through a novel pathway, EGFR/ERK1/2/FOXO3a/1/PGC-1α, under physiological and pathological conditions. As such, ERK1/2 down-regulates mitochondrial function directly by phosphorylation of upstream regulators of PGC-1α and subsequently decreasing MB.

ERK1/2 is a major player in various cell signaling pathways, including proliferation, differentiation, senescence, cell injury and recovery, and apoptosis. ERK1/2 becomes activated through a variety of extracellular stimuli, including receptor tyrosine kinases (RTK) such as the epidermal growth factor receptor (EGFR),[3] which leads to the activation of mitogen-activated protein kinase kinase (MEK) (1, 2). EGFR agonists activate intrinsic tyrosine kinase activity within the cytoplasmic domain of the receptor, initiating the recruitment of Ras, a GTPase, which allows for interaction with downstream effectors, including the Raf protein kinases. Raf phosphorylates MEK1/2, which phosphorylates ERK1/2. ERK1/2 is thought to be the only substrate for MEK1/2 phosphorylation, which has allowed for MEK1/2 inhibitors to be used specifically for ERK1/2 inactivation (3, 4).

ERK1/2 is also activated by cell stressors, including reactive oxygen species. In a study utilizing H_2O_2 injury in human renal cells, ERK1/2 inhibition was shown to decrease necrosis and apoptosis (5), whereas in a cisplatin-induced cell injury model, ERK1/2 inhibition reduced caspase 3 activation and apoptosis (6). In renal proximal tubular cells (RPTC), phosphorylated ERK1/2 was shown to reduce mitochondrial respiration and ATP production by decreasing complex I electron transport chain activity in response to *tert*-butyl hydroperoxide (TBHP), a model oxidant (7). Nowak *et al.* (7) also showed that expression of a constitutively active MEK1 increased ERK1/2 activation and decreased basal and uncoupled oxygen consumption, a measure of electron transport chain activity. Zhuang *et al.* (8) demonstrated that H_2O_2 treatment of RPTC led to a high level of ERK1/2 phosphorylation and loss of mitochondrial membrane potential, which was attenuated by treating with a MEK/ERK1/2 inhibitor. Finally, Fe^{2+}-induced mitochondrial swelling was shown to occur through activation of the ERK1/2 pathway (8). These findings illustrate that ERK1/2 decreases mitochondrial function in response to injury.

The kidney is a high energy-consuming organ, and its cells have an abundance of mitochondria to meet ATP demand, especially within the proximal tubules (9). Previous studies demonstrated that rapid and persistent disruption of mitochondria homeostasis is an important contributor to the pathology of renal ischemia/reperfusion (IR) injury (10, 11).

* This work was supported in part by National Institutes of Health NIGMS Grants GM084147 (to R. G. S.) and P20-GM103542-02 (to South Carolina Center of Biomedical Research Excellence (COBRE) in Oxidants, Redox Balance, and Stress Signaling), NIDDK (Grant F31DK105782 to J. B. C.); the National Institutes of Health National Center for Research Resources (Grant UL1-RR029882); the Biomedical Laboratory Research and Development Program of the Department of Veterans Affairs (Grant 5I01 BX-000851 to R. G. S.); and the South Carolina Clinical and Translational Research Institute at the Medical University of South Carolina. The authors declare that they have no conflicts of interest with the contents of this article. The content is solely the responsibility of the authors and does not necessarily represent the official views of the National Institutes of Health.

[1] Present address: University of Arizona, Drachman Hall, 1295 N. Martin Ave., P. O. Box 210202, Tucson, AZ 85721-02023.

[2] To whom correspondence should be addressed: University of Arizona, Drachman Hall, 1295 N. Martin Ave., POB 210202, Tucson, AZ 85721-02023. E-mail: schnell@pharmacy.arizona.edu

[3] The abbreviations used are: EGFR, epidermal growth factor receptor; MB, mitochondrial biogenesis; TBHP, *tert*-butyl hydroperoxide; RPTC, renal proximal tubule cell(s); IR, ischemia/reperfusion; AKI, acute kidney injury.

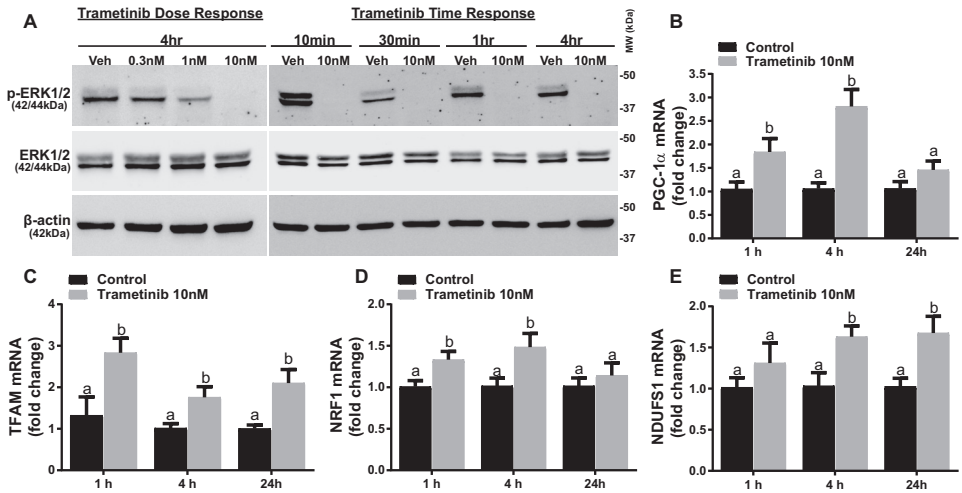

FIGURE 1. **ERK1/2 inhibition increases levels of PGC-1α and downstream targets of MB mRNA.** *A*, immunoblotting analysis of phosphorylated ERK1/2 (*p-ERK1/2*) in RPTC in response to increasing concentrations of trametinib at 4 h and increasing time of exposure to 10 nM trametinib. *Veh*, vehicle; *MW*, molecular weight. *B–E*, mRNA expression of PGC-1α, TFAM, NDUFS1, and NRF1 at 1, 4, and 24 h after treatment with 10 nM trametinib. Data are represented as mean ± S.E., $n \geq 5$. Different superscripts indicate statistically significant differences ($p < 0.05$).

Peroxisome proliferator-activated receptor γ coactivator-1α (PGC-1α) is thought to be the master regulator of mitochondria biogenesis (MB) and is enriched in tissues with high metabolic demand, such as the heart, skeletal muscle, and kidney (12, 13). The role of ERK1/2 activation and subsequent regulation of PGC-1α and downstream targets involved in mitochondrial homeostasis and dysfunction remains limited.

Physiological and pathological stimuli, such as exercise, caloric restriction, hypoxia, sepsis, and IR, are known to alter PGC-1α expression (9, 14). IR-induced renal injury rapidly suppresses MB, PGC-1α, and its direct downstream targets at the transcriptional and protein level (10, 11, 13). However, the mechanism(s) by which PGC-1α is transcriptionally suppressed after injury has not been determined. Therefore, we examined the role of ERK1/2 in renal PGC-1α transcription under physiological and pathophysiological conditions in primary cultures of RPTC and in the renal cortex of mice. We determined that ERK1/2 regulates PGC-1α in RPTC and in the renal cortex of mice at a physiological level through phosphorylation of the transcription factors forkhead box O3/1 (FOXO3a/1). EGFR was found to be the upstream activator of ERK1/2 under basal conditions, negatively regulating PGC-1α transcription. Finally, under the pathophysiological condition of IR-induced AKI in mice, ERK1/2 activation was responsible for the initial decrease in PGC-1α mRNA expression and the decrease in kidney function as measured by serum creatinine. By inhibiting ERK1/2 activation, we attenuated the early decrease in PGC-1α and prevented the decrease in kidney function. This research is significant because PGC-1α is the key regulator for MB, and by sustaining mitochondrial homeostasis, ERK1/2 inhibition may be a potential therapeutic to prevent further injury and/or increase recovery where early mitochondrial dysfunction is observed.

Results

ERK1/2 Inhibition Increases Levels of PGC-1α and Downstream Targets of MB mRNA in RPTC—To test the hypothesis that ERK1/2 regulates PGC-1α and MB at a physiological level, we utilized the pharmacological MEK1/2 inhibitor trametinib and primary cultures of rabbit RPTC. Trametinib has been well characterized as a potent and specific inhibitor of MEK1/2 with an IC_{50} of 0.92–3.4 nM in various cell lines and shows limited inhibitory activity against at least 98 other kinases (15, 16). RPTC were treated with 0.3, 1, or 10 nM trametinib, and at 10 nM trametinib, ERK1/2 phosphorylation was completely inhibited after 4 h (Fig. 1*A*). Trametinib (10 nM) completely inhibited ERK1/2 phosphorylation within 10 min and continued to inhibit it for 24 h (data not shown) without altering total ERK1/2 (Fig. 1*A*). PGC-1α mRNA expression increased 1.8-fold at 1 h and 2.8-fold at 4 h before decreasing to control levels at 24 h after trametinib exposure (Fig. 1*B*). The increase in PGC-1α mRNA was linked to increased nuclear encoded mediators of MB and gene targets of PGC-1α, including mitochondrial transcription factor A (TFAM), nuclear respiratory factor-1 (NRF1), and NADH dehydrogenase (ubiquinone) Fe-S protein 1 (NDUFS1) at 1, 4 and 24 h after trametinib treatment (Fig. 1, *C–E*). These results reveal that ERK1/2 represses PGC-1α mRNA expression and its downstream target genes under physiological conditions and that inhibition of ERK1/2 activation results in a rapid induction of PGC-1α mRNA and other downstream MB genes.

ERK1/2 Regulates PGC-1α through Phosphorylation of FOXO3a Independent of p38 and AKT Kinases in RPTC—We analyzed the phosphorylation levels of FOXO3a in RPTC 30 min after trametinib treatment because FOXO3a is a direct transcriptional regulator of PGC-1α (17–19). Phosphorylation of the ERK1/2 phosphorylation site, serine 294, on FOXO3a decreased 54% at 30 min in RPTC treated with trametinib (Fig. 2, *A* and *B*). Other kinases, such as p38 and AKT, are known to target FOXO3a for phosphorylation (20, 21); however, p38 and AKT phosphorylation did not change in the presence of trametinib (Fig. 2*C*).

To exert its transcriptional effects, FOXO3a shuttles between the cytosol and the nucleus (22). Phosphorylation of FOXO3a inactivates the protein by preventing it from entering the nucleus and increases the rate of export from the nucleus to

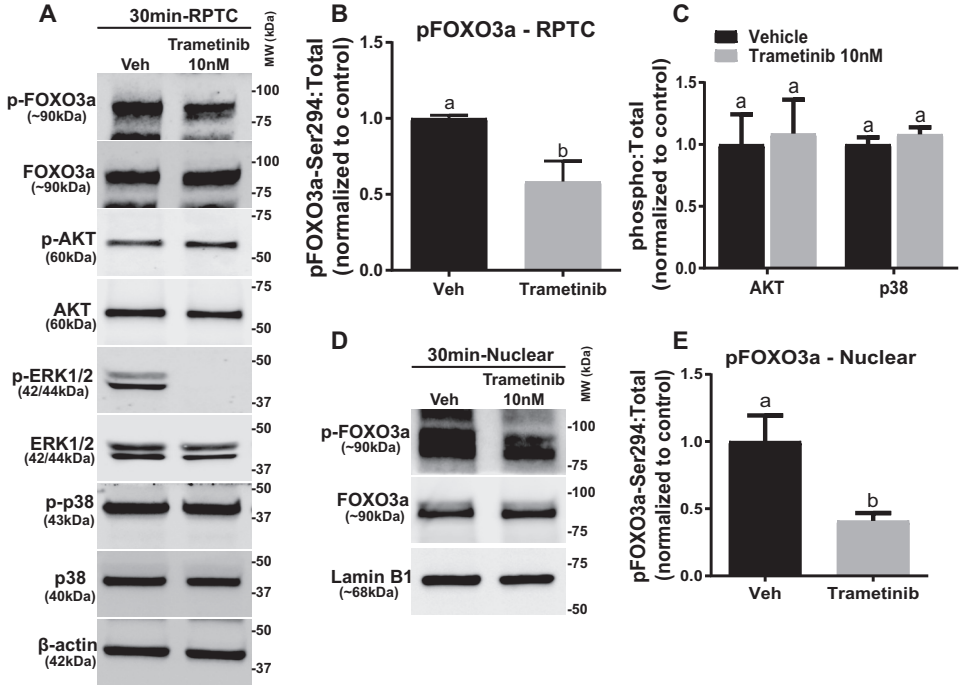

FIGURE 2. **ERK1/2 regulates PGC-1α through phosphorylation of FOXO3a independent of p38 and AKT kinases in RPTC.** *A*, representative immunoblot of pFOXO3a after 10 nM trametinib treatment in RPTC. *p*, phosphorylated; *Veh*, vehicle; *MW*, molecular weight. *B*, densitometry analysis of phosphorylated FOXO3a, with β-actin as loading control. *C*, densitometry analysis of p38 and AKT kinases. *D*, representative immunoblot of phosphorylated and total FOXO3a in the nucleus. *E*, densitometry analysis of phosphorylated FOXO3a in the nucleus following ERK1/2 inhibition. Data are represented as mean ± S.E., $n \geq 5$. Different superscripts indicate statistically significant differences ($p < 0.05$).

the cytosol, where it may be degraded (23). Therefore, phosphorylation of FOXO3a decreases its ability to bind to promoters and increase gene expression (20, 23, 24). Nuclear phosphorylated FOXO3a decreased 60% in the trametinib-treated RPTC at 30 min with no alteration in total FOXO3a nor the loading control, lamin B1 (Fig. 2, *D* and *E*). In summary, phosphorylated ERK1/2, but not AKT or p38, phosphorylates FOXO3a, which inactivates FOXO3a in the nucleus and prevents FOXO3a from increasing PGC-1α expression physiologically. This dynamic control of FOXO3a by ERK1/2 regulates PGC-1α, rapidly leading to a decrease/increase MB gene regulation.

EGFR Inhibition Increases PGC-1α mRNA Expression by Preventing ERK1/2 Activation in RPTC—EGFR is known to regulate the activity of the ERK1/2 signaling cascade (1, 25, 26). To determine whether ERK1/2 inhibition of PGC-1α mRNA was mediated by the EGFR in RPTC, we utilized the EGFR inhibitor erlotinib, a direct inhibitor of the intracellular kinase domain of the EGFR that prevents autophosphorylation and signal transduction (26). Within 1 h of erlotinib treatment (100 nM and 1 μM), ERK1/2 phosphorylation was blocked without a change in total ERK1/2 protein and remained decreased 4 h after treatment (Fig. 3*A*). PGC-1α mRNA expression was increased at 4 h by 2.4- and 2.8-fold in the 100 nM and 1 μM erlotinib groups, respectively (Fig. 3*B*). NRF1 was also up 2.4-fold by 4 h after EGFR inhibition (Fig. 3*C*). We conclude that EGFR inhibition with erlotinib leads to an up-regulation of PGC-1α mRNA through inactivation of ERK1/2. It should be noted that the 4-h increases in PGC-1α mRNA expression are very similar to the increases observed using trametinib (Fig. 1*B*). In summary, under physiological conditions, the activation of the EGFR/ERK1/2/FOXO3a pathway regulates PGC-1α and MB genes within 1 h.

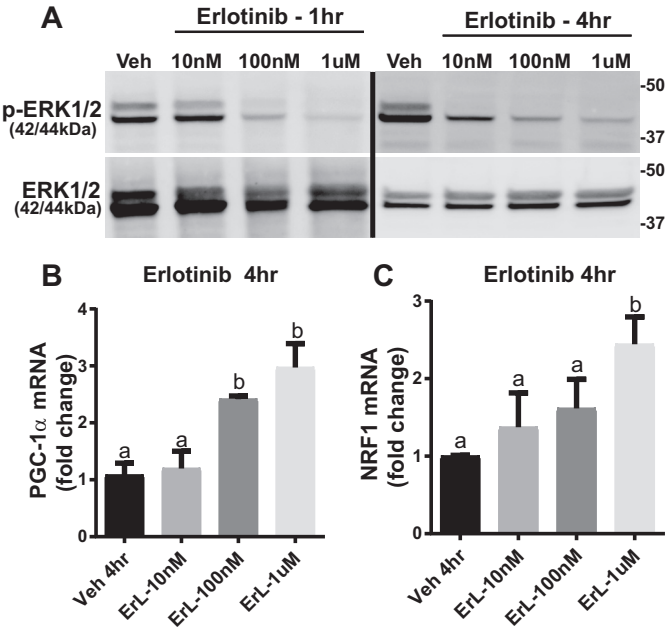

FIGURE 3. **EGFR inhibition increases PGC-1α mRNA expression by preventing ERK1/2 activation in RPTC.** *A*, representative immunoblot of phosphorylated ERK1/2 after treatment with increasing concentrations of erlotinib (*ErL*) at 1 and 4 h in RPTC. *p*, phosphorylated; *Veh*, vehicle. *B* and *C*, mRNA expression of PGC-1α (*B*) and NRF1 (*C*) following increasing concentrations of erlotinib at 4 h. Data are represented as mean ± S.E., $n \geq 5$. Different superscripts indicate statistically significant differences ($p < 0.05$).

ERK1/2 Physiologically Regulates PGC-1α Expression and Protein by Altering FOXO1 Phosphorylation in the Mouse Kidney—Our laboratory and others have previously reported that a 1 mg/kg dose of trametinib inhibits ERK1/2 phosphory-

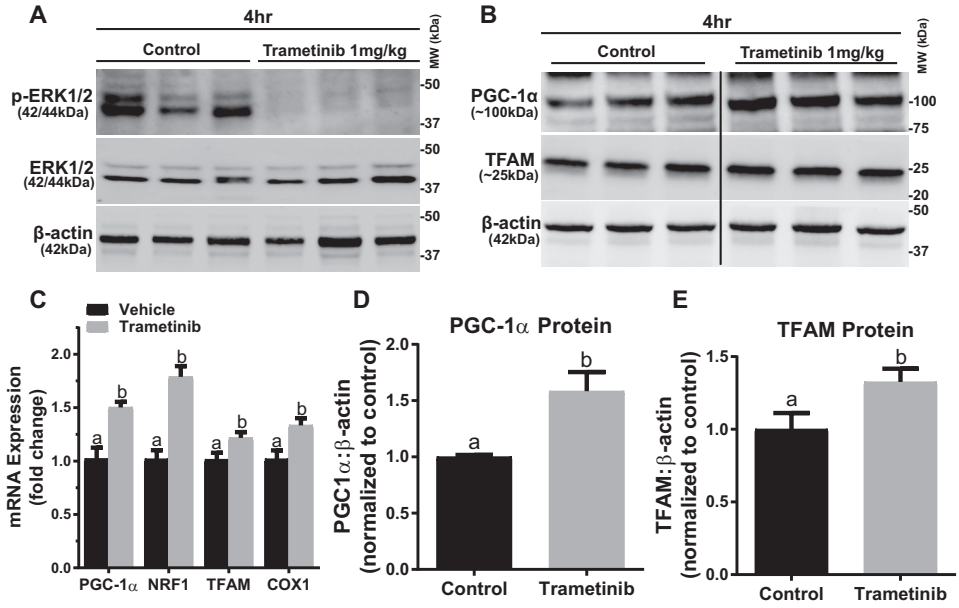

FIGURE 4. **ERK1/2 physiologically regulates PGC-1α expression and protein in mouse kidney.** *A*, representative immunoblot of phosphorylated ERK1/2 after treatment with trametinib in mouse kidney cortex. *p*, phosphorylated; *MW*, molecular weight. *B*, representative immunoblot of PGC-1α and TFAM proteins after treatment with trametinib in the kidney cortex. The *black line* represents the splicing of the blot from the same membrane. *C*, mRNA expression of PGC-1α, NRF1, TFAM, and COX 1 following trametinib administration at 4 h. *D* and *E*, densitometry analysis of PGC-1α (*D*) and TFAM (*E*) protein at 4 h following trametinib. Data are represented as mean ± S.E., $n \geq 5$. Different superscripts indicate statistically significant differences ($p < 0.05$).

lation in mice (16, 27). We verified that trametinib (1 mg/kg, i.p.) inhibited ERK1/2 phosphorylation at 4 h after injection in the renal cortex with no change to total ERK1/2 protein (Fig. 4*A*). PGC-1α mRNA expression in the renal cortex increased 1.5-fold 4 h after ERK1/2 inhibition, corresponding with the observations made *in vitro* (Fig. 2*C*). Likewise, targets of PGC-1α were also up-regulated at 4 h with NRF1 mRNA elevated by 1.8-fold and TFAM mRNA elevated by 1.2-fold (Fig. 2*C*). Cytochrome *c* oxidase I (COX1) mRNA, a mitochondrial encoded gene, one of the subunits of respiratory complex IV, was also up-regulated 1.4-fold following ERK1/2 inhibition with trametinib (Fig. 2*C*). The increase in MB gene expression due to ERK1/2 inhibition resulted in increases in PGC-1α and TFAM proteins of 1.6- and 1.3-fold, respectively, at 4 h in the trametinib group (Fig. 4, *B*, *D*, and *E*).

After failing to detect FOXO3a in the mouse renal cortex (data not shown), we examined FOXO1. FOXO3a and FOXO1 are similar transcription factors and share overlapping activities, including regulating PGC-1α (20). FOXO1 phosphorylation at the phosphorylation site, serine 329, was decreased in the trametinib group (28, 29) (Fig. 5, *A* and *B*). Total FOXO1 protein did not change in response to ERK1/2 inhibition (Fig. 5*A*). Neither AKT and p38 phosphorylation nor total AKT and p38 proteins changed in the trametinib group (Fig. 5*C*). Trametinib treatment decreased nuclear phosphorylated FOXO1 to total FOXO1 32%, 4 h after trametinib (Fig. 5, *D* and *E*). FOXO1 mRNA was also up-regulated at 4 h after ERK1/2 inhibition (Fig. 5*F*). Further evidence that ERK1/2 inhibition results in increased FOXO1 gene transcription was revealed by increases in catalase and mitochondrial superoxide dismutase 2 (SOD2), two genes regulated by FOXO1 (Fig. 5*F*) (30, 31). We conclude that ERK1/2 regulates the activity of FOXO1 within the nucleus and controls the basal level of PGC-1α mRNA and subsequent PGC-1α protein levels, as well as downstream MB genes in the kidney.

ERK1/2 Inhibition during AKI Attenuates an Increase in Serum Creatinine and Decreases in PGC-1α and NRF1 Expression—To examine the role of ERK1/2 on PGC-1α in the renal cortex under injurious conditions, we pretreated mice with trametinib or vehicle for 1 h and then subjected mice to bilateral IR surgery or sham surgery for 18 min to induce AKI; kidneys were collected 3 h later. IR-induced AKI decreases PGC-1α mRNA expression, as well as other mitochondrial genes and proteins (32). Trametinib prevented the increase in ERK1/2 phosphorylation following the IR (Fig. 6*A*). PGC-1α mRNA decreased 41% in IR mice after 3 h, and trametinib attenuated this decrease (Fig. 6*B*). Interestingly, trametinib pretreatment increased NRF1 expression following IR when compared with sham, whereas IR alone resulted in 13% decrease in NRF1 when compared with sham (Fig. 6*B*). At the protein level, both PGC-1α and TFAM proteins increased 1.7- and 2.4-fold, respectively (Fig. 6, *C* and *D*).

Serum creatinine, a marker of renal dysfunction, increased 4-fold in the IR group at 3 h and was attenuated in the trametinib pretreatment group (Fig. 6*E*). We demonstrate that by inhibiting ERK1/2 phosphorylation prior to inducing IR AKI, we attenuated the decreases in PGC-1α and NRF1 mRNA, as well as increasing mitochondrial related proteins PGC-1α and TFAM 3 h after surgery. By maintaining mitochondrial function due to ERK1/2 inhibition, kidney dysfunction was prevented at 3 h.

Erlotinib Blocks ERK1/2 Phosphorylation in Naive Mice and following IR, Preventing Decreases in PGC-1α and NRF1 Expression—To elucidate the role of EGFR on ERK1/2 and PGC-1α and MB genes in the renal cortex, erlotinib (50 mg/kg i.p.) was administered to naive mice (33). Erlotinib decreased

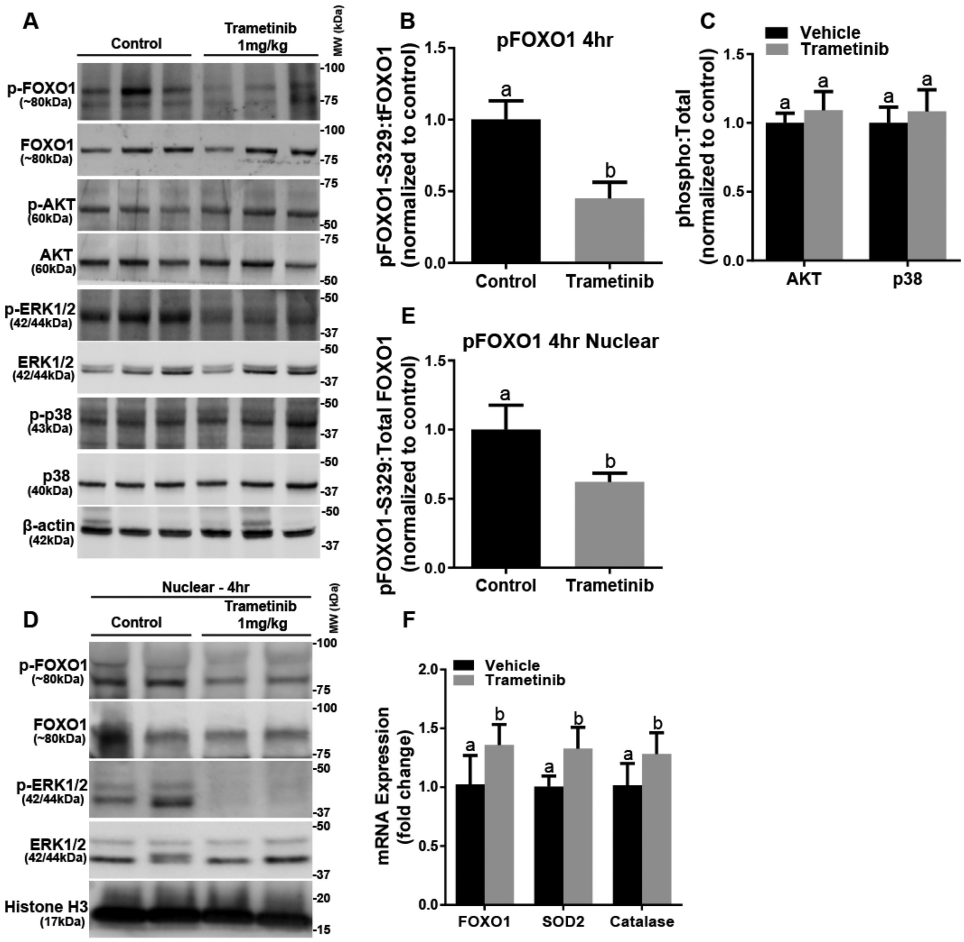

FIGURE 5. **FOXO1 phosphorylation in the cortex and nuclear phosphorylation decrease after ERK1/2 inhibition.** *A*, representative immunoblot of phosphorylated FOXO1 and ERK1/2, AKT, and p38 kinases following trametinib administration. *p*, phosphorylated; *MW*, molecular weight. *B*, densitometry analysis of phosphorylated FOXO1 when compared with total FOXO1. *C*, densitometry analysis of phosphorylated AKT to total AKT, and phosphorylated p38 to total p38 after trametinib treatment. *D*, representative immunoblot of nuclear phosphorylated FOXO1 and ERK1/2 after trametinib treatment in mouse kidney cortex. *E*, densitometry analysis of phosphorylated FOXO1 when compared with total FOXO1 after inhibition of ERK1/2 in the nucleus. *F*, mRNA expression of FOXO1, SOD2, and catalase at 4 h following trametinib administration. Data are represented as mean ± S.E., $n \geq 4$. Different superscripts indicate statistically significant differences ($p < 0.05$).

ERK1/2 phosphorylation by 45% in the kidney cortex 4 h after administration (Fig. 7, *A* and *B*). Mice given erlotinib had 1.3-fold higher PGC-1α mRNA and 1.4-fold higher FOXO1 mRNA expression (Fig. 7*C*). To elucidate whether the EGFR is the upstream receptor required for the ERK1/2 activation that down-regulates PGC-1α following IR AKI, we pretreated with erlotinib prior to inducing IR AKI. We observed attenuation in the increase of phosphorylated ERK1/2 at 3 h when compared with IR alone (Fig. 7, *D* and *E*). The results were very similar to those obtained in the trametinib experiments (Fig. 6, *B* and *C*); we observed attenuation of PGC-1α and NRF1 mRNA when compared with the IR group, as well as an increase in PGC-1α protein (Fig. 7, *F* and *G*). The erlotinib group also prevented the 5-fold increase in serum creatinine seen in the IR group (Fig. 7*H*). These data reveal that EGFR actively regulates ERK1/2 phosphorylation in the kidney, and as a consequence, EGFR regulates renal PGC-1α mRNA at a physiological and pathophysiological level. In summary, EGFR is the upstream receptor regulator of basal ERK1/2 phosphorylation in the renal cortex that controls PGC-1α mRNA and MB genes.

Discussion

In this study, we identified ERK1/2 as an important and rapid regulator of PGC-1α gene transcription in RPTC and in mouse kidney under physiological and pathological conditions. In RPTC, we showed that trametinib inhibits ERK1/2 phosphorylation within 10 min, leading to an increase in PGC-1α mRNA expression that was sufficient to up-regulate mitochondrial genes involved in MB. In addition, we determined that EGFR was the upstream activator of ERK1/2 in both RPTC and renal cortex. Thus, the EGFR/ERK1/2/FOXO(3a/1) pathway is an important negative regulator of PGC-1α and its downstream targets, including MB genes.

Previous studies revealed that ERK1/2 down-regulates mitochondrial function by decreasing basal and uncoupled oxygen consumption following TBHP exposure in RPTC (7). Furthermore, ATP production was reduced 40% in RPTC due to ERK1/2 activation by TBHP, and by inhibiting ERK1/2, ATP remained at control levels. In contrast, ERK1/2 inhibition was found to decrease ATP production and cause a rapid loss of mitochondrial membrane potential in alveolar macrophages

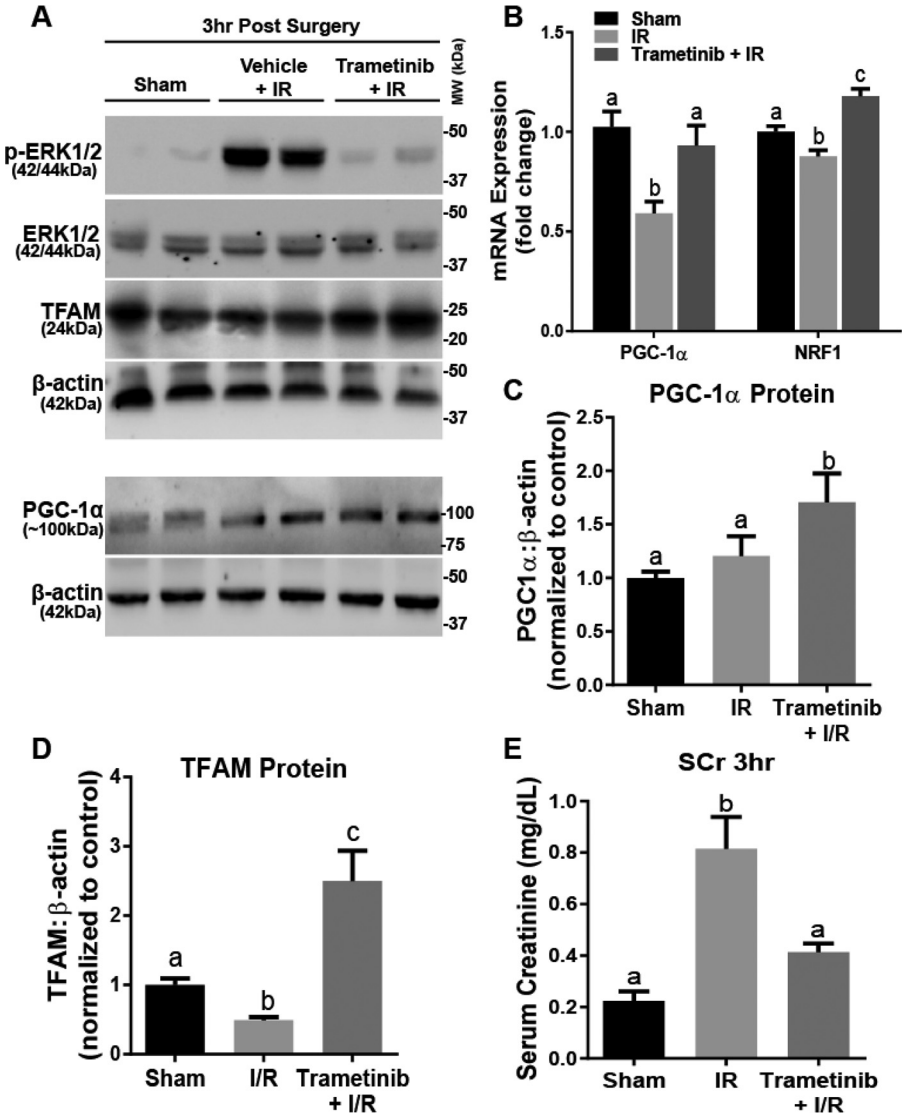

FIGURE 6. **ERK1/2 inhibition during AKI attenuates an increase in serum creatinine and increases PGC-1α and TFAM proteins.** *A*, representative immunoblot of phosphorylated ERK1/2, total ERK1/2, TFAM, and PGC-1α following IR AKI. *p*, phosphorylated; *MW*, molecular weight. *B*, mRNA expression of PGC-1α and NRF1 following IR AKI at 3 h after IR in the kidney cortex. *C* and *D*, densitometry analysis of PGC-1α (*C*) and TFAM (*D*) proteins following 3 h IR. *E*, serum creatinine was assessed 3 h after IR AKI. Data are represented as mean ± S.E., $n \geq 5$. Different superscripts indicate statistically significant differences ($p < 0.05$).

(34), but not in primary cultures of tracheobronchial epithelial cells or lung fibroblasts. A decrease in oxygen consumption through inhibition of complex I in HL-60 cells was found to occur by ERK1/2 inhibition (35). Overall, ERK1/2 decreases mitochondrial function by three mechanisms: 1) post-translational modifications that decrease electron transport chain activity, 2) down-regulation of PGC-1α and mitochondrial gene expression, and 3) decreased expression of mitochondrial protectants (*i.e.* SOD2). However, ERK1/2 appears to regulate mitochondrial functions differently in various cell types, and the differences may be based on the level of oxidative phosphorylation that occurs in each cell type. RPTC used by Nowak *et al.* (7) and in our studies derive all their energy from oxidative phosphorylation, similar to that found in kidney cortex.

In RPTC, FOXO3a phosphorylation was decreased 30 min after trametinib treatment. These results are consistent with previous studies that show ERK1/2 regulates phosphorylation of FOXO3a (23, 36). Phosphorylation is a key determinant of FOXO3a localization and its regulation of PGC-1α (37–39). Yang *et al.* (23) showed that ERK1/2 phosphorylation of FOXO3a promotes a FOXO3a degradation pathway mediated by the E3 ubiquitin ligase MDM2. We show that ERK1/2 inhibition decreased phosphorylated FOXO3a in the nucleus, allowing greater FOXO3a and PGC-1α expression physiologically. This FOXO3a-dependent increase in PGC-1α was also shown during endothelial oxidative stress (19).

It is not clear the exact pathways that regulate ERK1/2 during basal conditions in RPTC. In experiments using the specific EGFR inhibitor erlotinib, ERK1/2 phosphorylation was blocked and PGC-1α mRNA was increased. Thus, EGFR appears to be a key regulator of ERK1/2, which in turn regulates the basal level of PGC-1α mRNA and its downstream mitochondrial genes. Nevertheless, it remains to be determined what is activating the EGFR under these conditions. Possible candidates

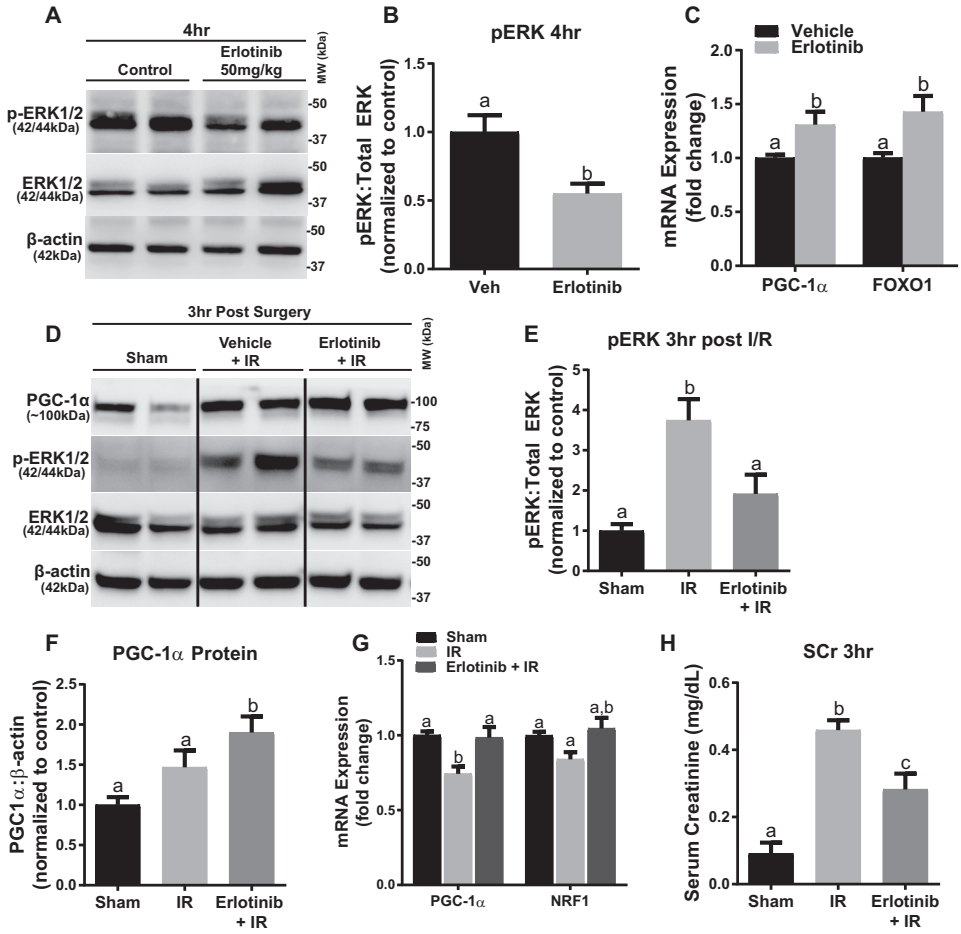

FIGURE 7. **Erlotinib blocks ERK1/2 phosphorylation in naïve mice and following IR, preventing decreases in PGC-1α and NRF1 expression.** *A*, representative immunoblot of phosphorylated ERK1/2 after 4 h of treatment with erlotinib in mouse kidney cortex. *p*, phosphorylated; *MW*, molecular weight. *B*, densitometry analysis of phosphorylated ERK1/2 when compared with total ERK1/2 following 4 h of erlotinib treatment. *C*, mRNA expression of PGC-1α and FOXO1 at 4 h in mouse cortex following erlotinib treatment. *D*, representative immunoblot of phosphorylated ERK1/2 and total ERK1/2, as well as PGC-1α following IR AKI. *E*, densitometry analysis of phosphorylated ERK1/2 when compared with total ERK1/2 following 3 h of IR AKI. *F*, densitometry analysis of PGC-1α protein when compared with β-actin following 3 h of IR AKI. *G*, mRNA expression of PGC-1α and NRF1 following 3 h of IR AKI. *H*, serum creatinine was assessed 3 h after IR AKI. Data are represented as mean ± S.E., $n \geq 4$. Different superscripts indicate statistically significant differences ($p < 0.05$).

include EGFR ligands, TGFα and HB-EGF (heparin-binding EGF-like growth factor), and/or transactivation pathways (ADAM17, ANGII (angiotensin II), TWEAK/Fn14) (4, 40).

Inhibiting ERK1/2 increased PGC-1α mRNA, as well as TFAM, NRF1, and COX1. The increase in COX1 demonstrates that ERK1/2 is increasing not only nuclear encoded gene expression, but also mitochondrial encoded gene expression. This response is similar to findings in melanoma cell lines after treatment with various ERK cascade inhibitors in which an increase in PGC-1α gene expression was observed (41).

Because FOXO3a was not expressed in naive mouse renal cortex, we shifted our focus to FOXO1. FOXO3a and FOXO1 share similar DNA-binding domains, have overlapping gene expressions (42), and are both directly phosphorylated by ERK1/2 (43). Phosphorylation of FOXO1 decreased in the nucleus due to ERK1/2 inhibition, which resulted in an increase in downstream targets of FOXO1 (*e.g.* catalase and SOD2) and PGC-1α in the kidney cortex.

During IR-induced AKI in mice, ERK1/2 is highly phosphorylated with accompanying decreases in PGC-1α and NRF1, as well as a decline in kidney function at 3 h after IR surgery. Inhibiting phosphorylated ERK1/2 pre-surgery attenuated the PGC-1α and NRF1 mRNA decreases and prevented an increase in serum creatinine. We have previously shown that PGC-1α is rapidly decreased following diverse models of AKI in mice and rats, and these results implicate ERK1/2 as the mediator behind this transcriptional suppression (10, 11, 32).

In conclusion, we determined the role of ERK1/2 in the physiological and pathological regulation of renal PGC-1α and MB. We linked EGFR activation and FOXO3a/1 inactivation to the down-regulation of PGC-1α and MB, through ERK1/2 signaling. PGC-1α physiological regulation appears to be structured so that changes can occur very rapidly when necessary. Finally, ERK1/2 inhibition may have potential in preventing mitochondrial dysfunction as a therapeutic strategy in organ dysfunction. Because mitochondrial injury/recovery and biogenesis can occur throughout different tissues of the body due to various injury insults, we think this therapeutic potential of inhibiting early activation of ERK1/2 to prevent down-regulation of MB may be applicable to other organs. Further studies will be required to investigate this therapeutic potential.

TABLE 1
Mouse primer sequence pairs with forward (F) and reverse (R) primers identified

Gene	F/R	Primer sequences
PGC-1α	F	5′-AGGAAATCCGAGCGGAGCTGA
	R	5′-GCAAGAAGGCGACACATCGAA
FOXO1	F	5′-CGGAAAATCACCCCGGAGAA
	R	5′-TACACCAGGGAATGCACGTC
NRF1	F	5′-TCGGGCATTTATCCCAGAGATGCT
	R	5′-TACGAGATGAGCTATACTGTGTGT
SOD2	F	5′-ACACATTAACGCGCAGATCA
	R	5′-AGCCTCCAGCAACTCTCCTT
NDUFS1	F	5′-AGATGATTTGGGAACAACAG
	R	5′-TAAGGCTTAGAGGTTAGGGC
COX1	F	5′-ACCATCATTTCTCCTTCTCC
	R	5′-GGTGGGTAGACTGTTCATCC
TFAM	F	5′-GCTGATGGGTATGGAGAAG
	R	5′-GAGCCGAATCATCCTTTGC
Catalase	F	5′-TCACTGACGAGATGGCACAC
	R	5′-ATCGAACGGCAATAGGGGTC
Actin	F	5′-GGGATGTTTGCTCCAACCAA
	R	5′-GCGCTTTTGACTCAGGATTTAA

TABLE 2
Rabbit primer sequence pairs with forward (F) and reverse (R) primers identified

Gene	F/R	Primer sequences
PGC-1α	F	5′-CGCAAAGAGTACGAGAAGCG
	R	5′-AGCTGTCTCCATCATCCCG
NRF1	F	5′-CACCTACACTGAGCACAGCA
	R	5′-TTGGACTCGAACACGTGAGG
NDUFS1	F	5′-AGATGATTTGGGAACAACAG
	R	5′-TAGGGCTTAGAGGTTAGAGC
TFAM	F	5′-TGCGCCTCACCTTTCAGTTT
	R	5′-CTCCACAGCTCGGCAATTCT
Tubulin	F	5′-CTCTCTGTCGATTACGGCAAG
	R	5′-TGGTGAGGATGGAGTTGTAGG

Experimental Procedures

In Vitro Studies—Female New Zealand White rabbits (2 kg) were purchased from Charles River (Oakwood, MI). RPTC were isolated using the iron oxide perfusion method and grown in 35-mm tissue culture dishes under improved conditions similar to what is observed *in vivo*, as described previously (44). The culture medium was a 1:1 mixture of Dulbecco's modified Eagle's medium/F-12 (without glucose, phenol red, or sodium pyruvate) supplemented with 15 mM HEPES buffer, 2.5 mM L-glutamine, 1 μM pyridoxine HCl, 15 mM sodium bicarbonate, and 6 mM lactate. Hydrocortisone (50 nM), selenium (5 ng/ml), human transferrin (5 μg/ml), bovine insulin (10 nM), and L-ascorbic acid-2-phosphate (50 μM) were added to fresh culture medium. Confluent RPTC were used for all experiments. RPTC monolayers were treated with various compounds or vehicle (DMSO) for the time points indicated.

In Vivo Studies—Trametinib (GSK1120212, (15)) was purchased from Selleck Chemicals (Houston, TX). 8-to-9-week-old male C57BL/6 mice (20–25 g) mice received an injection of trametinib (1 mg/kg i.p.) or vehicle control (DMSO). 4 h after injection, kidneys were collected and flash-frozen for further analysis.

Mice were assigned to three groups: 1) sham, 2) I/R + vehicle, and 3) I/R + trametinib. Vehicle or trametinib was administered i.p. 1 h before surgery. I/R mice were subjected to I/R surgery by bilateral renal pedicle clamping for 18 min as described previously (32). Briefly, the renal artery and vein were isolated and blood flow was occluded with a vascular clamp for 18 min while maintaining a constant body temperature of 36–37 °C. Sham mice were treated exactly the same as I/R mice without the clamping of the renal pedicles. Mice were euthanized at 3 h after surgery, and blood and kidneys (flash-frozen in liquid nitrogen) were collected for analysis.

Quantitative Reverse Transcription PCR Analysis of mRNA Expression—Total RNA was isolated from renal cortical tissue with TRIzol reagent (Life Technologies). The iScript Advanced cDNA Synthesis Kit (Bio-Rad) was used according to the manufacturer's protocol. The generated cDNA was used with the SsoAdvanced Universal SYBR Green Supermix reagent (Bio-Rad). The relative mRNA expression of all genes was determined by the $2-\Delta\Delta Ct$ method, and mouse actin RNA and rabbit tubulin RNA were used as reference genes for normalization (see Tables 1 and 2 for primer pairs).

Immunoblotting Analysis—Protein was extracted from renal cortex using radioimmunoprecipitation assay buffer (50 mM Tris-HCl, 150 mM NaCl, 0.1% SDS, 0.5% sodium deoxycholate, 1% Triton X-100, pH 7.4) with protease inhibitor cocktail (1:100), 1 mM sodium fluoride, and 1 mM sodium orthovanadate (Sigma-Aldrich). Mouse tissue and rabbit primary cells nuclear and cytosolic fraction lysates were prepared as described previously with modifications (11). Briefly, a piece of kidney cortex was homogenized in sucrose isolation buffer (250 mM sucrose, 1 mM EGTA, 10 mM HEPES, 1 mg/ml fatty acid-free BSA (pH 7.4)) with a Dounce tissue grinder. Lysates were centrifuged at 1000 × *g* for 10 min. The first pellet was rewashed two separate times in isolation buffer and resuspended in radioimmunoprecipitation assay. The first supernatant was centrifuged at 10,000 × *g* for 5 min for further purification of the cytosol fraction. Histone H3 and/or lamin B1 were used as loading control for nuclear lysate immunoblots, and α-tubulin was used for loading control of cytosolic lysates.

Equal protein quantities (20–60 μg) were loaded onto 4–15% SDS-PAGE gels, resolved by gel electrophoresis, and transferred onto nitrocellulose or PVDF membranes (Bio-Rad). Membranes were blocked in 5% bovine serum albumin or 5% milk in Tris buffered saline solution with Tween (TBST) and incubated overnight with primary antibody at 4 °C with gentle agitation. Primary antibodies used in these studies included phospho-ERK1/2 (1:1000) (#4370), total ERK1/2 (1:1000) (#4695), AKT (1:1000) (#9272), phospho-AKT (1:1000) (#4060), phospho-p38 (1:1000) (#4511), p38 MAPK (1:1000) (#8690), EGF receptor (1:1000) (#4267), phospho-EGFR Tyr-1173 (1:750) (#4407s), phospho-EGFR Tyr-1068 (1:1000) (#3777s), total FOXO3a (1:1000), phospho-Ser-294-FOXO3a (1:1000) (#5538), total FOXO1 (1:1000) (#2880), and histone H3 (1:2000) (#9715), all from Cell Signaling Technology, Danvers, MA; phospho-Ser-329-FOXO1 (1:1000) (ab192201), TFAM (1:1000) (ab131607), lamin B1 (1:1000) (ab16048), and PGC-1α (1:1000) (ab54481), all from Abcam; kidney injury molecule-1 (KIM-1) (1:1000; AF1817), from R&D Systems, Minneapolis, MN; and β-actin (1:2000) (sc-47778), from Santa Cruz Biotechnology, Dallas, TX.

Membranes were incubated with the appropriate horseradish peroxidase-conjugated secondary antibody before visualization using enhanced chemiluminescence (Thermo Scientific) and the GE ImageQuant LAS4000 (GE Life Sciences). Optical density was determined using the ImageJ software from the National Institutes of Health.

Statistical Analysis—All data are shown as mean ± S.E. When comparing two experimental groups, an unpaired, two-tailed *t* test or Mann-Whitney U was used to determine statistical differences. A one-way analysis of variance followed by Tukey's post hoc test was performed for comparisons of multiple groups. $p < 0.05$ was considered statistically significant. All statistical tests were performed using the GraphPad Prism software (GraphPad Software, San Diego, CA).

Author Contributions—J. B. C. and R. G. S. created the conceptualization and methodology and wrote the original draft; J. B. C. was responsible for the formal analysis; J. B. C. and R. M. W. performed the investigation; S. T. E. and R. G. S. reviewed and edited the manuscript; J. B. C. and R. G. S. performed data visualization; and R. G. S. was responsible for the funding acquisition.

Acknowledgments—Animal facilities were funded by the National Institutes of Health National Center for Research Resources (Grant C06-RR015455).

References

1. Daub, H., Weiss, F. U., Wallasch, C., and Ullrich, A. (1996) Role of transactivation of the EGF receptor in signalling by G-protein-coupled receptors. *Nature* **379,** 557–560
2. Luttrell, L. M., Della Rocca, G. J., van Biesen, T., Luttrell, D. K., and Lefkowitz, R. J. (1997) Gβγ subunits mediate Src-dependent phosphorylation of the epidermal growth factor receptor: a scaffold for G protein-coupled receptor-mediated Ras activation. *J. Biol. Chem.* **272,** 4637–4644
3. Wortzel, I., and Seger, R. (2011) The ERK cascade: distinct functions within various subcellular organelles. *Genes Cancer* **2,** 195–209
4. Forrester, S. J., Kawai, T., O'Brien, S., Thomas, W., Harris, R. C., and Eguchi, S. (2016) Epidermal growth factor receptor transactivation: mechanisms, pathophysiology, and potential therapies in the cardiovascular system. *Annu. Rev. Pharmacol. Toxicol.* **56,** 627–653
5. Sabbatini, M., Santillo, M., Pisani, A., Paternò, R., Uccello, F., Serù, R., Matrone, G., Spagnuolo, G., Andreucci, M., Serio, V., Esposito, P., Cianciaruso, B., Fuiano, G., and Avvedimento, E. V. (2006) Inhibition of Ras/ERK1/2 signaling protects against postischemic renal injury. *Am. J. Physiol. Renal Physiol.* **290,** F1408–F1415
6. Nowak, G. (2002) Protein kinase C-α and ERK1/2 mediate mitochondrial dysfunction, decreases in active Na^+ transport, and cisplatin-induced apoptosis in renal cells. *J. Biol. Chem.* **277,** 43377–43388
7. Nowak, G., Clifton, G. L., Godwin, M. L., and Bakajsova, D. (2006) Activation of ERK1/2 pathway mediates oxidant-induced decreases in mitochondrial function in renal cells. *Am. J. Physiol. Renal Physiol.* **291,** F840–F855
8. Zhuang, S., Kinsey, G. R., Yan, Y., Han, J., and Schnellmann, R. G. (2008) Extracellular signal-regulated kinase activation mediates mitochondrial dysfunction and necrosis induced by hydrogen peroxide in renal proximal tubular cells. *J. Pharmacol. Exp. Ther.* **325,** 732–740
9. Lameire, N. H., Bagga, A., Cruz, D., De Maeseneer, J., Endre, Z., Kellum, J. A., Liu, K. D., Mehta, R. L., Pannu, N., Van Biesen, W., and Vanholder, R. (2013) Acute kidney injury: an increasing global concern. *Lancet* **382,** 170–179
10. Stallons, L. J., Funk, J. A., and Schnellmann, R. G. (2013) Mitochondrial homeostasis in acute organ failure. *Curr. Pathobiol. Rep.* **1,** 169–177
11. Funk, J. A., and Schnellmann, R. G. (2013) Accelerated recovery of renal mitochondrial and tubule homeostasis with SIRT1/PGC-1α activation following ischemia-reperfusion injury. *Toxicol. Appl. Pharmacol.* **273,** 345–354
12. Scarpulla, R. C. (2008) Transcriptional paradigms in mammalian mitochondrial biogenesis and function. *Physiol. Rev.* **88,** 611–638
13. Puigserver, P., and Spiegelman, B. M. (2003) Peroxisome proliferator-activated receptor-γ coactivator 1 α (PGC-1 α): transcriptional coactivator and metabolic regulator. *Endocr. Rev.* **24,** 78–90
14. Che, R., Yuan, Y., Huang, S., and Zhang, A. (2014) Mitochondrial dysfunction in the pathophysiology of renal diseases. *Am. J. Physiol. Renal Physiol.* **306,** F367–F378
15. Gilmartin, A. G., Bleam, M. R., Groy, A., Moss, K. G., Minthorn, E. A., Kulkarni, S. G., Rominger, C. M., Erskine, S., Fisher, K. E., Yang, J., Zappacosta, F., Annan, R., Sutton, D., and Laquerre, S. G. (2011) GSK1120212 (JTP-74057) is an inhibitor of MEK activity and activation with favorable pharmacokinetic properties for sustained *in vivo* pathway inhibition. *Clin. Cancer Res.* **17,** 989–1000
16. Yamaguchi, T., Kakefuda, R., Tajima, N., Sowa, Y., and Sakai, T. (2011) Antitumor activities of JTP-74057 (GSK1120212), a novel MEK1/2 inhibitor, on colorectal cancer cell lines *in vitro* and *in vivo*. *Int. J. Oncol.* **39,** 23–31
17. Borniquel, S., García-Quintáns, N., Valle, I., Olmos, Y., Wild, B., Martínez-Granero, F., Soria, E., Lamas, S., and Monsalve, M. (2010) Inactivation of Foxo3a and subsequent downregulation of PGC-1 α mediate nitric oxide-induced endothelial cell migration. *Mol. Cell. Biol.* **30,** 4035–4044
18. Daitoku, H., Yamagata, K., Matsuzaki, H., Hatta, M., and Fukamizu, A. (2003) Regulation of PGC-1 promoter activity by protein kinase B and the forkhead transcription factor FKHR. *Diabetes* **52,** 642–649
19. Olmos, Y., Valle, I., Borniquel, S., Tierrez, A., Soria, E., Lamas, S., and Monsalve, M. (2009) Mutual dependence of Foxo3a and PGC-1α in the induction of oxidative stress genes. *J. Biol. Chem.* **284,** 14476–14484
20. Tzivion, G., Dobson, M., and Ramakrishnan, G. (2011) FoxO transcription factors; regulation by AKT and 14-3-3 proteins. *Biochim. Biophys. Acta* **1813,** 1938–1945
21. Ho, K. K., McGuire, V. A., Koo, C. Y., Muir, K. W., de Olano, N., Maifoshie, E., Kelly, D. J., McGovern, U. B., Monteiro, L. J., Gomes, A. R., Nebreda, A. R., Campbell, D. G., Arthur, J. S., and Lam, E. W. (2012) Phosphorylation of FOXO3a on Ser-7 by p38 promotes its nuclear localization in response to doxorubicin. *J. Biol. Chem.* **287,** 1545–1555
22. Schachter, T. N., Shen, T., Liu, Y., and Schneider, M. F. (2012) Kinetics of nuclear-cytoplasmic translocation of Foxo1 and Foxo3A in adult skeletal muscle fibers. *Am. J. Physiol. Cell Physiol.* **303,** C977–C990
23. Yang, J. Y., Zong, C. S., Xia, W., Yamaguchi, H., Ding, Q., Xie, X., Lang, J. Y., Lai, C. C., Chang, C. J., Huang, W. C., Huang, H., Kuo, H. P., Lee, D. F., Li, L. Y., Lien, H. C., *et al.* (2008) ERK promotes tumorigenesis by inhibiting FOXO3a via MDM2-mediated degradation. *Nat. Cell Biol.* **10,** 138–148
24. Tseng, A. H., Wu, L. H., Shieh, S. S., and Wang, D. L. (2014) SIRT3 interactions with FOXO3 acetylation, phosphorylation and ubiquitinylation mediate endothelial cell responses to hypoxia. *Biochem. J.* **464,** 157–168
25. Pierce, K. L., Luttrell, L. M., and Lefkowitz, R. J. (2001) New mechanisms in heptahelical receptor signaling to mitogen activated protein kinase cascades. *Oncogene* **20,** 1532–1539
26. Raymond, E., Faivre, S., and Armand, J. P. (2000) Epidermal growth factor receptor tyrosine kinase as a target for anticancer therapy. *Drugs* **60,** Suppl. 1, 15–23; discussion 41–12
27. Smith, J. A., Stallons, L. J., Collier, J. B., Chavin, K. D., and Schnellmann, R. G. (2015) Suppression of mitochondrial biogenesis through Toll-like receptor 4-dependent mitogen-activated protein kinase kinase/extracellular signal-regulated kinase signaling in endotoxin-induced acute kidney injury. *J. Pharmacol. Exp. Ther.* **352,** 346–357
28. Zhao, Y., Wang, Y., and Zhu, W. G. (2011) Applications of post-translational modifications of FoxO family proteins in biological functions. *J. Mol. Cell Biol.* **3,** 276–282
29. Woods, Y. L., Rena, G., Morrice, N., Barthel, A., Becker, W., Guo, S., Unterman, T. G., and Cohen, P. (2001) The kinase DYRK1A phosphorylates the transcription factor FKHR at Ser^{329} *in vitro*, a novel *in vivo* phosphorylation site. *Biochem. J.* **355,** 597–607

30. Sengupta, A., Molkentin, J. D., Paik, J. H., DePinho, R. A., and Yutzey, K. E. (2011) FoxO transcription factors promote cardiomyocyte survival upon induction of oxidative stress. *J. Biol. Chem.* **286,** 7468–7478
31. Greer, E. L., and Brunet, A. (2005) FOXO transcription factors at the interface between longevity and tumor suppression. *Oncogene* **24,** 7410–7425
32. Funk, J. A., and Schnellmann, R. G. (2012) Persistent disruption of mitochondrial homeostasis after acute kidney injury. *Am. J. Physiol. Renal Physiol.* **302,** F853–F864
33. Friess, T., Scheuer, W., and Hasmann, M. (2006) Erlotinib antitumor activity in non-small cell lung cancer models is independent of HER1 and HER2 overexpression. *Anticancer Res.* **26,** 3505–3512
34. Monick, M. M., Powers, L. S., Barrett, C. W., Hinde, S., Ashare, A., Groskreutz, D. J., Nyunoya, T., Coleman, M., Spitz, D. R., and Hunninghake, G. W. (2008) Constitutive ERK MAPK activity regulates macrophage ATP production and mitochondrial integrity. *J. Immunol.* **180,** 7485–7496
35. Ripple, M. O., Kim, N., and Springett, R. (2013) Acute mitochondrial inhibition by mitogen-activated protein kinase/extracellular signal-regulated kinase kinase (MEK) 1/2 inhibitors regulates proliferation. *J. Biol. Chem.* **288,** 2933–2940
36. Roy, S. K., Srivastava, R. K., and Shankar, S. (2010) Inhibition of PI3K/AKT and MAPK/ERK pathways causes activation of FOXO transcription factor, leading to cell cycle arrest and apoptosis in pancreatic cancer. *J. Mol. Signal.* **5,** 10
37. Van Der Heide, L. P., Hoekman, M. F., and Smidt, M. P. (2004) The ins and outs of FoxO shuttling: mechanisms of FoxO translocation and transcriptional regulation. *Biochem. J.* **380,** 297–309
38. Puigserver, P., Rhee, J., Donovan, J., Walkey, C. J., Yoon, J. C., Oriente, F., Kitamura, Y., Altomonte, J., Dong, H., Accili, D., and Spiegelman, B. M. (2003) Insulin-regulated hepatic gluconeogenesis through FOXO1-PGC-1alpha interaction. *Nature* **423,** 550–555
39. Link, W., Oyarzabal, J., Serelde, B. G., Albarran, M. I., Rabal, O., Cebriá, A., Alfonso, P., Fominaya, J., Renner, O., Peregrina, S., Soilán, D., Ceballos, P. A., Hernández, A. I., Lorenzo, M., Pevarello, P., *et al.* (2009) Chemical interrogation of FOXO3a nuclear translocation identifies potent and selective inhibitors of phosphoinositide 3-kinases. *J. Biol. Chem.* **284,** 28392–28400
40. Rayego-Mateos, S., Morgado-Pascual, J. L., Sanz, A. B., Ramos, A. M., Eguchi, S., Batlle, D., Pato, J., Keri, G., Egido, J., Ortiz, A., and Ruiz-Ortega, M. (2013) TWEAK transactivation of the epidermal growth factor receptor mediates renal inflammation. *J. Pathol.* **231,** 480–494
41. Haq, R., Shoag, J., Andreu-Perez, P., Yokoyama, S., Edelman, H., Rowe, G. C., Frederick, D. T., Hurley, A. D., Nellore, A., Kung, A. L., Wargo, J. A., Song, J. S., Fisher, D. E., Arany, Z., and Widlund, H. R. (2013) Oncogenic BRAF regulates oxidative metabolism via PGC1α and MITF. *Cancer Cell* **23,** 302–315
42. Furuyama, T., Nakazawa, T., Nakano, I., and Mori, N. (2000) Identification of the differential distribution patterns of mRNAs and consensus binding sequences for mouse DAF-16 homologues. *Biochem. J.* **349,** 629–634
43. Asada, S., Daitoku, H., Matsuzaki, H., Saito, T., Sudo, T., Mukai, H., Iwashita, S., Kako, K., Kishi, T., Kasuya, Y., and Fukamizu, A. (2007) Mitogen-activated protein kinases, Erk and p38, phosphorylate and regulate Foxo1. *Cell. Signal.* **19,** 519–527
44. Nowak, G., and Schnellmann, R. G. (1996) L-Ascorbic acid regulates growth and metabolism of renal cells: improvements in cell culture. *Am. J. Physiol.* **271,** C2072–C2080